# Evaluation of analysis technologies for gas diffusion

Author: Nozomi Okamoto    Toho Gas Co., Ltd., Nagoya, Japan
Joint authors:
Hisatoshi Ito    Toho Gas Co., Ltd., Nagoya, Japan
Ryuichi Tominaga, Hibiki Ryuzaki    Tokyo Gas Co., Ltd., Tokyo, Japan
Koichi Nishimura, Hideki Okamoto    Osaka Gas Co., Ltd., Osaka, Japan

Key word:
security of supply, new technology, new skill

# 1. Background

Knowing how gases mix and diffuse is important to gas utilities. For some time now, they had been obtaining this information via testing. In recent years, as computers have increased their processing speeds and come down in price, numerical analyses have become more sophisticated and a number of commercial software applications capable of fluid analyses of gas mixing and diffusion phenomena have been released.

In the near future numerical analysis could potentially replace experimentation as a means for understanding gas mixing and diffusion behavior.

Presently, the three gas utilities of Tokyo Gas, Osaka Gas and Toho Gas are using computational fluid dynamics (CFD) capable of three-dimensionally analyzing the distribution of gas concentration, to identify gas diffusion behavior.

CFD analysis identifies fluid phenomena by dividing a target space into a mesh structure of tiny cells and solving numerous fluid equations for these cells. Unless the mesh is subdivided into a higher number of cells, the desired accuracy is not obtained in the event of sudden changes in physical quantities such as fluid velocity. Inversely, however, a higher number of cells increases computation time and costs, therefore the mesh must be of an adequate definition. CFD tools incorporate a number of turbulence models, which must be carefully selected according to the phenomena. Moreover, boundary conditions at medium inlets and outlets have complicated velocity profiles and time histories, but since these conditions cannot be accurately set, appropriate modeling is necessary and this modeling readily impacts the accuracy of numerical analysis. And, for the phenomena of gas mixing and diffusion analysis handled by the gas utilities, a satisfactory guideline for the modeling has not been obtained.

# 2. Aims

Given this background, the three gas utilities of Tokyo Gas, Osaka Gas and Toho Gas are jointly working on establishing technology (guideline for the modeling) for estimating gas diffusion behavior.

To establish this technology (guideline for the modeling), they are analyzing gas mixing and diffusion behavior using three different CFD tools and comparing results against empirical data as a means for verifying tool accuracy.

Moreover, because full-scale experimenting presents difficulties in verifying tool accuracy, full-scale tests were reproduced on a bench scale and the similarity law has been tested to see whether it can be used to verify full-scale phenomena.

CFD analysis is capable of analysis in a three-dimensional space, but because of the massive amount of computations, analysis can take anywhere from a few days to a few

weeks. The gas utilities are, therefore, also looking to develop a fast analysis tool that enables faster analyses.

## 3. Methods

### 3.1 Bench Scale Test Method

The simulation of indoor gas diffusion assumes that methane gas is sprayed at an average flow velocity of $U = 1.02$ m/s from a nozzle of a diameter of $d = 20.8$ mm located in the center of the floor in a $21$ $m^3$ space ($L = 3.4$, $W = 2.56$, $H = 2.4$ m) comparable to a room, mixes with air as it diffuses and then escapes to the outside through openings near the ceiling. When the ventilation effect is taken into account, the air enters from openings near to the floor ($D = 0.005$ m, $L_S = 3.08$ m, cross-sectional area = $0.0154$ $m^2$) at an average flow velocity of $0.23$ m/s and it is assumed that a wooden home in Japan is ventilated 0.6 time/h on average. Full-scale tests, however, are not practical because they take time and money. Therefore, verifications are done by reproducing the full-scale phenomena on a bench scale of 1/8. The gas flowrate and ventilation rate are set according to the similarity law described in 3.3, so that the Richardson number $R_i = 0.155$ and flow rate ratio $b = 0.22$ would be the same as the full-scale phenomena. The methane gas density is $r_g = 0.68$ $kg/m^3$ and the air density was $r_a = 1.22$ $kg/m^3$.

The test conditions are given in Table 1 and the test system is shown in Fig. 1. In tests, a nozzle of a *2.6 mm* inner diameter standing *10 mm* above the floor is set in the center of a *32 x 42 x 30 cm* box, and methane gas is released from a high pressure bottle at a constant rate using a massflow controller (MQV9500BSSN0000D0, Yamatake). Separate tests are done without ventilation and with ventilation. In tests with ventilation, fresh air is supplied at a constant rate using a massflow controller (MQV0002BSSN0000D0, Yamatake) from a slit of *W 0.625 x D 385 mm* in size at the bottom of one wall and released via a slit of the same dimensions at the top of the opposite wall. Tests are kept to *about 30 min* in length to ensure that methane did not exceed the 5% lower flammability limit concentration.

Methane concentration is measured in a total of 54 points (horizontal 9 points x vertical 6 points) in the box as shown in Fig. 2. Data is logged at 4-minute intervals and concentration is analyzed by thermal conductivity detection using a gas chromatograph (Micro GC 490-GC, Varian).

Gas is absorbed by the gas chromatograph at a rate of *2.38 mL/min*, which is small compared to the injected gas quantity and air quantity, therefore it has little impact on tests.

Sampling time is offset by a *60 s* time lag in order to compensate for the time required for sampled gas to travel via the sampling pipe from the sampling port to the gas chromatograph, and the analysis time required by the gas chromatograph.

Table 1 The test conditions

| | unit | Bench-scale | Actual scale |
|---|---|---|---|
| Height of Box | mm | 300 | 2400 |
| Width of Box | mm | 320 | 2550 |
| Length of Box | mm | 425 | 3400 |
| Volume | | 40.32L | 20.8m3 |
| Diameter of Methane gas flow exit | mm | 2.6 | 20.8 |
| Width of Air flow Slit | mm | 0.625 | 5 |
| velocity of Methane gas flow | m/s | 0.36 | 1.02 |
| velocity of Air flow | m/s | 0.08 | 0.23 |
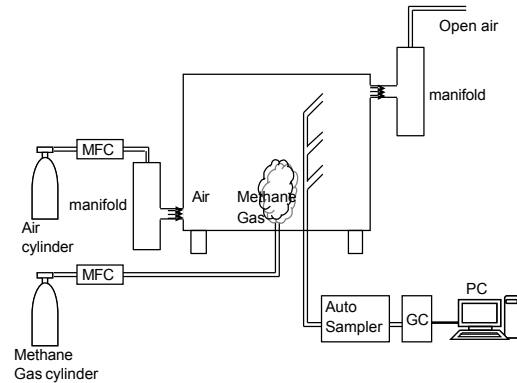


Figure 1 The test systems
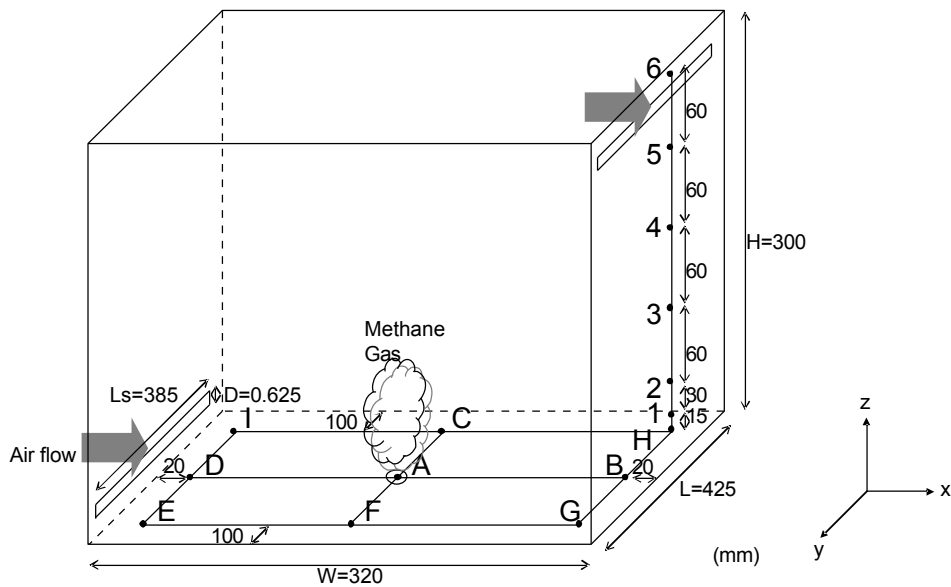


Figure 2 The test conditions

(A-I: measured points in the horizontal direction

1-6; measured points in the vertical direction)

## 3.2 Fundamental Equations for CFD Computations

The governing equations for gas mixing and diffusion behavior in the case of stratification consist of the following equation of continuity, mass conversion law as applied to methane, Navier-Stokes equations and average density equation.

Cases with turbulence add the $k - \varepsilon$ standard model equation often used in practical calculations.

Consideration is given to buoyancy caused by the difference in density between methane and air. The initial indoor state has the space filled with air at a pressure of *0 Pa* and still. At the gas nozzle outlet, gas is supplied at the gas flowrate or the average gas flow velocity obtained by dividing the flowrate by the nozzle cross-sectional area. At the ventilation inlet, the air flowrate or the average air flow velocity obtained by dividing the flowrate by the ventilation port area is given. At the ventilation outlet, pressure is a constant *0 Pa*. Walls have a viscous condition for cases of laminar flow and a wall function for cases of turbulence, while flux is 0 for the methane mass fraction.

$\langle$ governing equations $\rangle$

(equation of continuity)

$$\frac{\partial \rho}{\partial t} + div(\rho \mathbf{v}) = 0 \qquad \qquad \cdots(\text{Eq.1})$$

(mass conversion law as applied to methane)

$$\rho \frac{\partial Y}{\partial t} + \rho \mathbf{v}\, gradY = div(\rho D_i\, gradY) \qquad \cdots(\text{Eq.2})$$

(Navier-Stokes equations)

$$\rho \frac{\partial \mathbf{v}}{\partial t} + \rho \mathbf{v}\, grad(\mathbf{v}) = -gradP + \mu_g \Delta \mathbf{v} - (\rho - \rho_a)\mathbf{g} \qquad \cdots(\text{Eq.3})$$

(average density equation)

$$\rho = \rho_g X + \rho_a(1-X), \quad M = M_g X + M_a(1-X), X = \frac{M}{M_g}Y \qquad \cdots(\text{Eq.4})$$

$\langle$initial condition$\rangle$

$\rho = \rho_a$

$\mathbf{v} = 0$

$P = 0$

$Y = 0$

⟨boundary condition⟩

wall　　　　　　　　：　$\mathbf{v} = 0$　　$gradY = 0$

gas nozzle outlet：　$w = U = \dfrac{Q_g}{\mathrm{p}d^2/4}$　　$\mathrm{r} = \mathrm{r}_g$　　$Y = 1$

ventilation inlet　：　$u = U_v = \dfrac{Q_v}{L_s D}$

ventilation outlet　：　$P = 0$

## 3.3 Similarity Law

In order to reproduce full-scale phenomena in bench scale tests, the supply rate of methane and air are determined according to the similarity law.

The indoor length $L$ is given as the representative dimension, the gas average flow velocity U at the gas nozzle is given as the representative flow velocity and $L/U$ is the representative time. The equation is dimensionless at a pressure $\mathrm{r}_g U^2$ and density $\mathrm{r}_g$. A nondimensional parameter adds a superscript *.

⟨ nondimensional ⟩

$$x = Lx*　　　　　　　　　　　\cdots(\text{Eq.5})$$
$$y = Ly*　　　　　　　　　　　\cdots(\text{Eq.6})$$
$$z = Lz*　　　　　　　　　　　\cdots(\text{Eq.7})$$
$$t = \frac{L}{U}t*　　　　　　　　　　\cdots(\text{Eq.8})$$
$$\mathbf{v} = U\mathbf{v}*　　　　　　　　　　\cdots(\text{Eq.9})$$
$$P = \left(\mathrm{r}_g U^2\right)P*　　　　　　　\cdots(\text{Eq.10})$$
$$\mathrm{r} = \mathrm{r}_g \mathrm{r}*　　　　　　　　　　\cdots(\text{Eq.11})$$
$$M = M_g M*　　　　　　　　　\cdots(\text{Eq.12})$$

A dimensionless equation is obtained as shown below by substituting Equations 5 through 12 into Equations 1 through 4. However, g* is a unit vector for the vertical direction.

< dimensionless equation >

$$\frac{\partial r*}{\partial t*} + div(r * \mathbf{v}*) = 0 \qquad \cdots \text{(Eq.13)}$$

$$r * \frac{\partial Y}{\partial t*} + r * \mathbf{v} * gradY = \frac{1}{S_c \cdot R_e} div(r * gradY) \qquad \cdots \text{(Eq.14)}$$

$$r * \frac{\partial \mathbf{v}*}{\partial t*} + r * \mathbf{v} * grad\mathbf{v}* = -gradP* + \frac{\Delta \mathbf{v}*}{R_e} - R_i(r*-1)\mathbf{g}* \qquad \cdots \text{(Eq.15)}$$

$$r* = X + a(1-X), \quad M* = X + a(1-X), \quad X = M*Y \qquad \cdots \text{(Eq.16)}$$

< initial condition >

$r* = a$

$\mathbf{v}* = 0$

$P* = 0$

$Y = 0$

< boundary condition >

wall                    : $\mathbf{v}* = 0$    $gradY = 0$

gas nozzle outlet    : $w* = 1$    $r* = 1$    $Y = 1$

ventilation inlet      : $u* = b$,   $Y = 0$

ventilation outlet     : $P* = 0$

From the dimensionless equation and boundary conditions, there are five parameters in the Richardson number $R_i$, Reynolds number $R_e$, Schmidt number $S_c$, density ratio $\alpha$ and flow velocity ratio $\beta$. As long as these five parameters are equal, the same phenomena can be reproduced on any scale.

< five parameters >

$$R_i = \frac{(r_g - r_a)gL}{r_g U^2} \qquad \cdots \text{(Eq.17)}$$

$$R_e = \frac{r_g U L}{m_g} \qquad \cdots \text{(Eq.18)}$$

$$S_c = \frac{m_g}{D_i} \qquad \cdots \text{(Eq.19)}$$

$$a = \frac{r_a}{r_g} \qquad \cdots (Eq.20)$$

$$b = \frac{U_v}{U} \qquad \cdots (Eq.21)$$

There is not a specific bench scale at which all conditions were satisfied, but the Reynolds number was sufficiently large enough at 53200 under the full-scale condition and 2350 under the bench scale condition, therefore the far-right expression in each Equations 18 and 19 can be ignored. Accordingly, the Reynolds number and Schmidt number can be ignored, therefore it was decided to use a bench scale of 1/8 where the remaining three parameters were in agreement. The density ratio is the same for the bench scale and full scale, therefore gas flow velocity and ventilation flow velocity are determined with just two parameters: the Richardson number and flow velocity ratio.

## 4. Results

4.1 Benchmarks for the Three Utilities

Gas diffusion was analyzed under the same conditions as empirical tests using the CFD tools of each of the utilities (hereinafter referred to as "Case, 1, 2 and 3"). The accuracy of simulations was then measured by comparing those findings against the results from the bench scale tests. The simulation models of each of the utilities are given in Table 2.

Table2　The simulation models of each of the utilities

|  | Case1 | Case2 | Case3 |
|---|---|---|---|
| Total elements | 65,268 | 774,592 (in consideration of symmetry) | 1,184,754 |
| Time step | $5.78 \times 10\text{-}3\text{sec}$ | 0.05sec | 1sec |
| Turbulence model | k-$\varepsilon$ | - | - |

The CFD tools in all three cases are based on the finite volume method. Case1 can only build orthogonal cell meshes, while Case2 uses hex cell meshes and Case3 uses a mix of hex and tetra cell meshes. Case1 has considerably less cells in its meshes than the other tools, but the time steps are short. As such, the number of mesh cells and time steps were set with each tool, in consideration of simulation stability and computation time. Moreover, since the other two tools use a laminar model while Case1 does not have this capability, a $k - \varepsilon$ standard model was used for turbulence. Case2 targets half

the modeling area in consideration of symmetry.

Empirical results for tests without ventilation and benchmark results for each of the CFD tools are given in Figs. 3 and 4. In these figures, the points are at a height of 165 mm on the weak concentration points (B and C), and the transition in methane concentration is mostly linear. If simulation results are compared against empirical results, the error is about 8%. Empirical results for tests with ventilation are given in Figs. 5 and 6. With ventilation ongoing, methane concentration gradually rises. When simulation results are compared against empirical results, the error is about 10%. Figures 7 through 9 show the methane concentration and flowrate vectors after 30 minutes, for the respective CFD tools. Looking at the distribution of methane concentration, the concentration is evenly stratified in the horizontal direction. This stratification phenomenon was reported by Marshall et al. after conducting methane and air mixing and diffusion tests at various scales and under various conditions. That same phenomenon was confirmed here. Moreover, based on the flowrate vectors, methane sprayed from the nozzle reaches the ceiling without diffusing, then slowly flows downward. It is understood that, with any of the CFD tools, roughly the same test results can be reproduced by appropriately setting the physical model, mesh and time step.
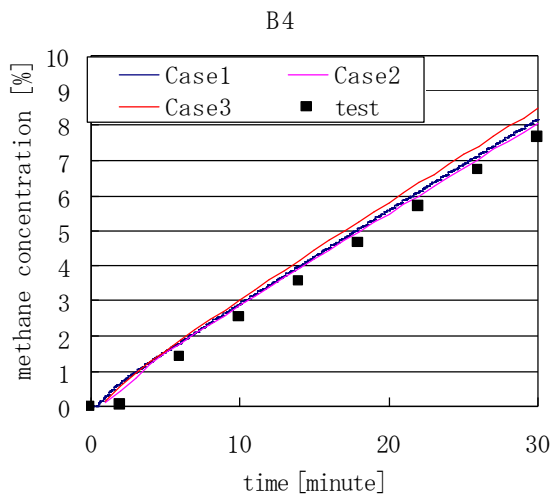
Figure 3 Benchmark results of each CFD tool under the conditions without ventilation
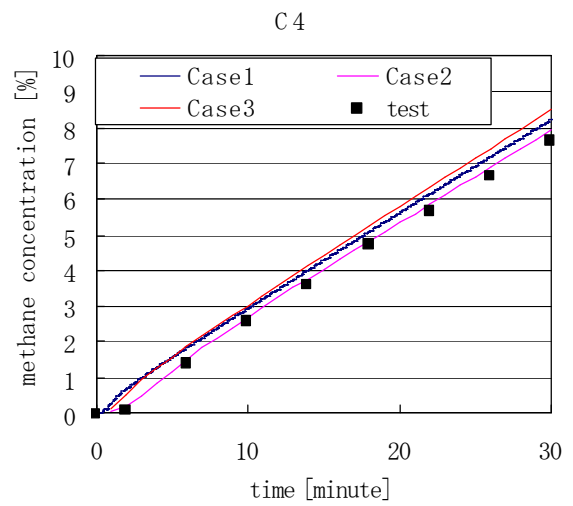


Figure 4 Benchmark results of each CFD tool under the conditions without ventilation
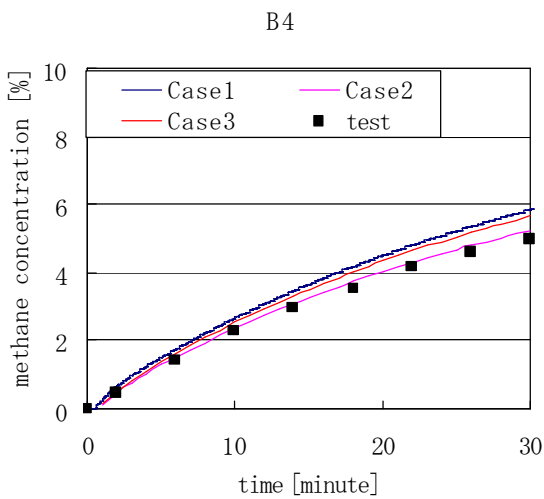


Figure 5 Benchmark results of each CFD tool under the conditions with ventilation
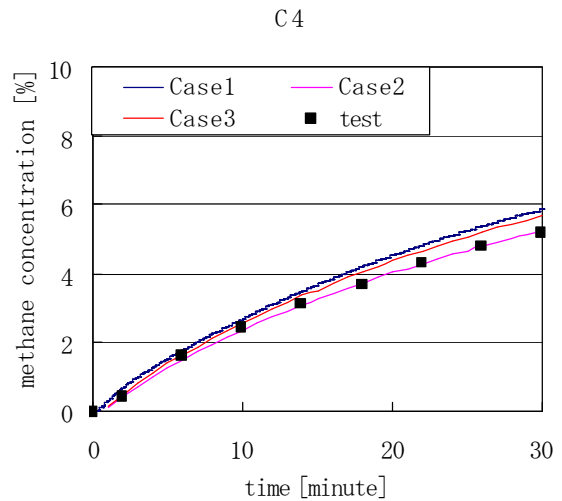


Figure 6 Benchmark results of each CFD tool under the conditions with ventilation
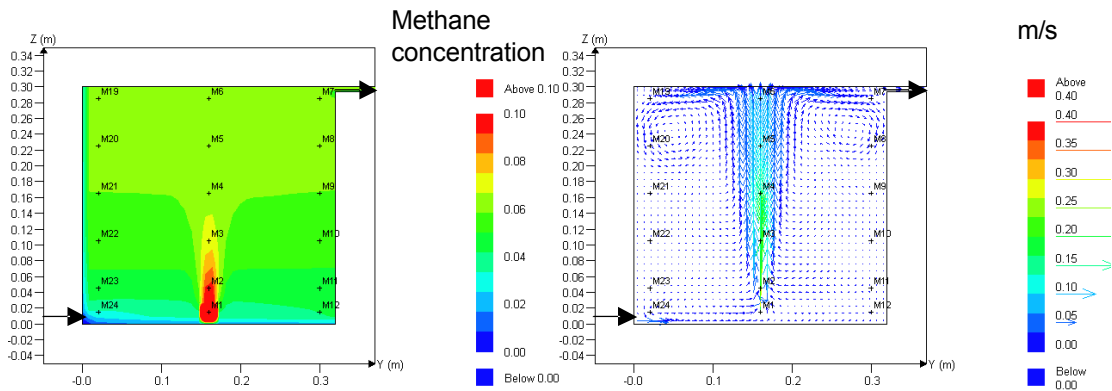
Figure 7 Methane concentration(Left) and flowrate vectors(Right) after 30 minutes
(Case1)
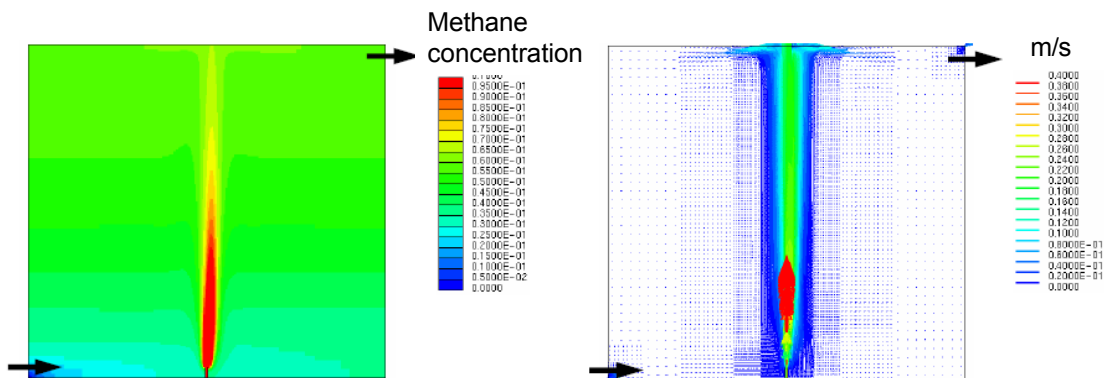


Figure 8 Methane concentration(Left) and flowrate vectors(Right) after 30 minutes
(Case2)
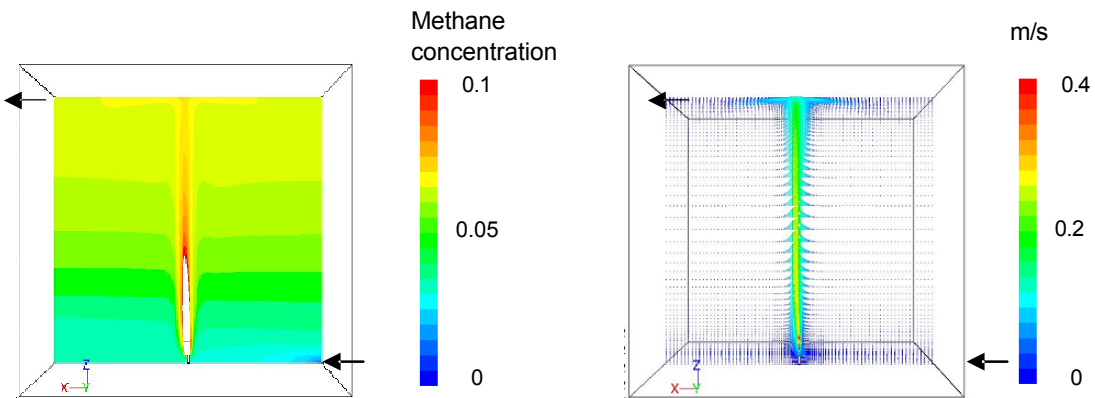


Figure9 Methane concentration(Left) and flowrate vectors(Right) after 30 minutes
(Case3)

## 4.2 Verification of Similarity Law

To verify whether the assumptions of the similarity law are correct or not, comparisons were done of the full-scale computation results, bench scale empirical results and bench scale computation results.

The simulation model of the full-scale computations is given in Table 3. With Case1 and Case3, the scale number  is large, therefore the mesh and computation step are changed. Moreover, the Reynolds of the physical model is large, therefore computations with all three CFD tools was done using a $k - \varepsilon$ model.

Table 3    The simulation model of the full-scale computations

|  | Case1 | Case2 | Case3 |
|---|---|---|---|
| Total elements | 79,560 | 774,592 (in consideration of symmetry ) | 60,200 |
| Time step | 9.57 × 10-3sec | 0.05sec | 5sec |
| Turbulence model | k- $\varepsilon$ | k- $\varepsilon$ | k- $\varepsilon$ |

If results are the same when compared using dimensionless amounts, then the similarity law holds true. Here, concentration is dimensionless, therefore comparisons are done with a dimensionless time component in line with the similarity law.

$$t = \left( L/U \right) \cdot t * \qquad\qquad \cdots\text{(Eq.22)}$$

The dimensionless time component of Equation 22 is given in Table 4.

Table 4    The dimensionless time component

| Actual time [min] | Actual time [sec] | dimensionless time of the full -scale | dimensionless time of the bench scale |
|---|---|---|---|
| 10 | 600 | 255.3 | 722.9 |
| 30 | 1800 | 7666.0 | 2168.7 |
| 50 | 3000 | 1276.6 | 3614.4 |
| 70 | 4200 | 1787.2 | 5060.2 |
| 90 | 5400 | 2297.9 | 6506.0 |

A comparison of the full-scale computation results using each of the CFD tools, the bench scale computation results and the bench scale empirical results is shown in Fig. 10. From this figure, it can be seen that the results from the three Cases using the differing CFD tools are roughly the same, thus the similarity law holds true. And, since the similarity law was verified as applicable, bench scale empirical results are recognized as verifying full-scale phenomena.
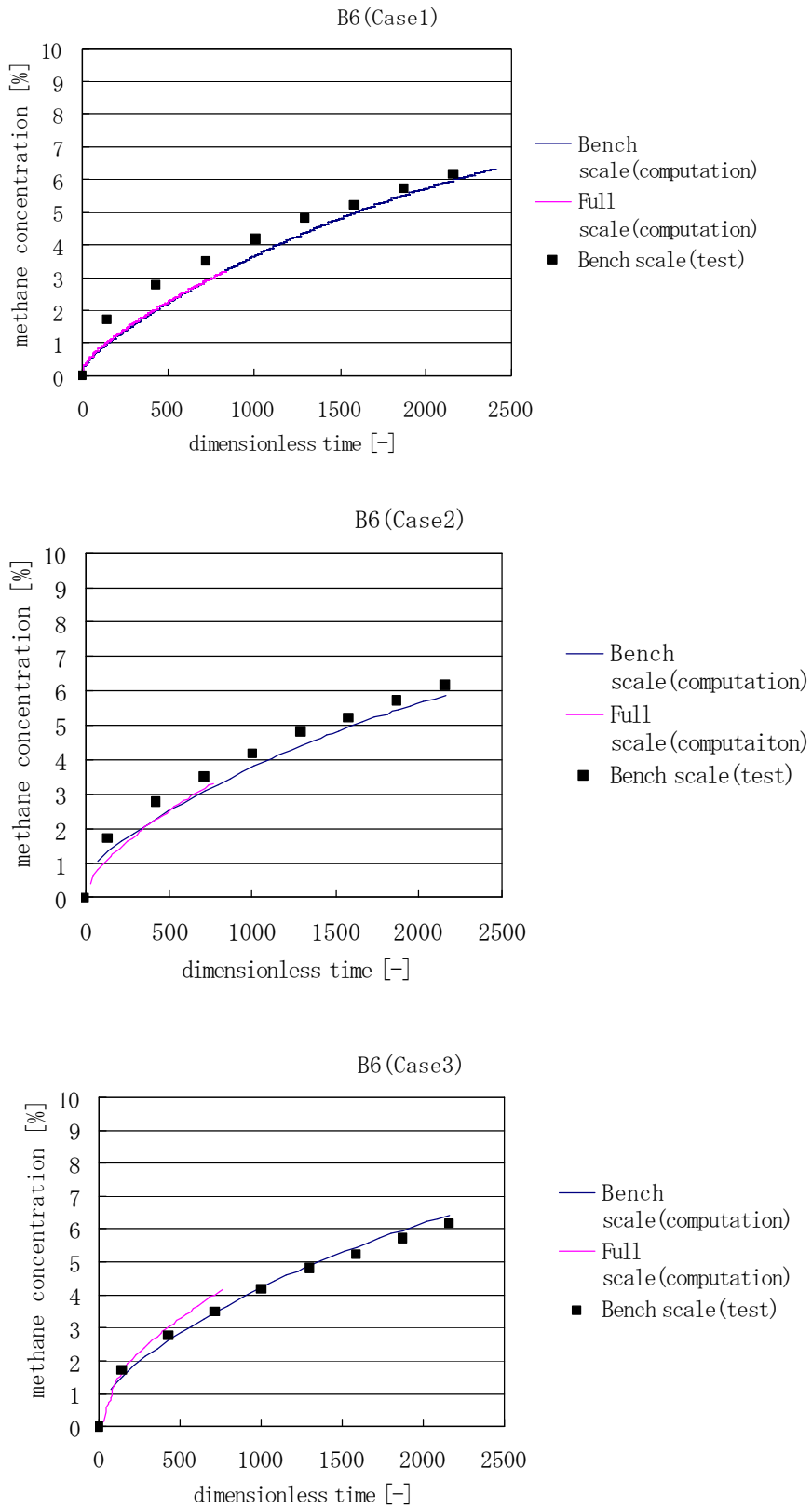
Figure10  Verification of Similarity Law

## 4.3 Fast Analysis Tool

It is understood from CFD analysis results that methane concentration is mostly uniform in the horizontal direction. Given this, analyses could thinkably be simpler and quicker than CFD by estimating just the concentration profile in the vertical direction. With that in mind, a one-dimensional model for estimating the concentration profile in the vertical direction is created and made into a computational tool.

The created one-dimensional model applied the theory of G. Worster et al.: if a gas of lesser density than the gas filling a closed space is sprayed upward from the floor into that space, the buoyant turbulence plume mixes with surrounding gas as it rises to the ceiling. After that, the gas mixture flows downward from the ceiling surface to the walls. As long as the turbulence plume does not flow at a fast rate, the concentration field stratifies into a one-dimensional vertical profile. G. Worster et al. obtained an asymptotic solution for the time history of the concentration profile.

Since the G. Worster's theory is modeled without ventilation, the one-dimensional model was improved for application to computations with ventilation. Equations 23 through 29 are the governing equations of this one-dimensional model.

The difference from G. Worster's theory is Equation 26, as it takes into consideration the convection current of ventilation air entering from the floor.

⟨ dimensionless equation （applied the theory of G. Worster）⟩

(Law of conservation concerning jet volume)

$$\frac{d}{dz}\int_0^\infty \overline{w}\,2\mathrm{p}r\,dr = 2\mathrm{p}Ebw \qquad\qquad \cdots (Eq.23)$$

(Law of conservation concerning jet motion)

$$\frac{d}{dz}\int_0^\infty \mathrm{r}_a\overline{w}^2\,2\mathrm{p}r\,dr = \int_0^\infty (\mathrm{r}_0 - \mathrm{r})g\,2\mathrm{p}r\,dr \qquad\qquad \cdots (Eq.24)$$

(Law of conservation concerning jet mass)

$$\frac{d}{dz}\int_0^\infty \mathrm{r}\,\overline{w}\,2\mathrm{p}r\,dr = 2\mathrm{p}E\mathrm{r}_0bw \qquad\qquad \cdots (Eq.25)$$

(Law of conservation concerning indoor gas mixture mass without jet)

$$\frac{\partial \mathrm{r}_0}{\partial t} + \frac{\partial (\mathrm{r}_0 U - nH)}{\partial z} = -\frac{2\mathrm{p}E\mathrm{r}_0bw}{A} \qquad\qquad \cdots (Eq.26)$$

(Boundary density)

$$t = 0 : \mathsf{r}_0 = \mathsf{r}_a \qquad\qquad \cdots (\text{Eq.27})$$

(Boundary conditions of jet outlet)

$$z = 0 : Q = \mathsf{p}b^2 w, \frac{Q^2}{\mathsf{p}d^2} = \frac{\mathsf{p}b^2 w^2}{2}, \frac{\mathsf{r}_a - \mathsf{r}_g}{\mathsf{r}_a} Qg = \frac{\mathsf{p}b^2 w \Delta}{2} \qquad\qquad \cdots (\text{Eq.28})$$

(Boundary conditions of ceiling)

$$z = H : \overline{w} = 0 \qquad\qquad \cdots (\text{Eq.29})$$

The below simplified equation is created because the flowrate distribution and concentration profile when injecting a gas that is lighter than air can be approximated as a Gaussian distribution.

$$\overline{w}(z,r) = w(z) \exp(-\frac{r^2}{b^2}) \qquad\qquad \cdots (\text{Eq.30})$$

$$\{\mathsf{r}_0 - \mathsf{r}(z,r)\}g = \mathsf{r}_1 \Delta(z) \exp(-\frac{r^2}{b^2}) \qquad\qquad \cdots (\text{Eq.31})$$

Accordingly, the governing equation can be expressed as follows.

$$\frac{d}{dz}\left(b^2 w\right) = 2Ebw \qquad\qquad \cdots (\text{Eq.32})$$

$$\frac{d}{dz}\left(\frac{b^2 w}{2}\right) = b^2 \Delta \qquad\qquad \cdots (\text{Eq.33})$$

$$\frac{d}{dz}\left(\frac{b^2 w \Delta}{2}\right) = b^2 w \frac{\partial \Delta_0}{\partial z} \qquad\qquad \cdots (\text{Eq.34})$$

$$\frac{\partial \Delta_0}{\partial t} = \left(\frac{\mathsf{p}b^2 w}{A} - nA\right)\frac{\partial \Delta_0}{\partial z} \qquad\qquad \cdots (\text{Eq.35})$$

$$z = 0 : Q = \mathsf{p}b^2 w, \frac{Q^2}{\mathsf{p}d^2} = \frac{\mathsf{p}b^2 w^2}{2}, \frac{\mathsf{r}_a - \mathsf{r}_g}{\mathsf{r}_a} Qg = \frac{\mathsf{p}b^2 w \Delta}{2} \qquad\qquad \cdots (\text{Eq.36})$$

$$t = 0, z = H : \Delta_0 = 0.5\Delta \qquad\qquad \cdots (\text{Eq.37})$$

$$t = 0, 0 \leq z < H : \Delta_0 = 0 \qquad\qquad \cdots (\text{Eq.38})$$

A tool has been developed for numerically integrating the aforementioned governing equation. The developed fast analysis tool is compared against empirical data and analytical results from the three CFD tools to verify its accuracy. As shown in Table 5, the conditions for verification are to diffuse methane gas into a 32 x 42 x 30 cm box that

is ventilated at a rate of 1.7 time/h. The entrainment coefficient is E = 0.875, based on plume experiments by Papanicolaou et al.

Table 5 the conditions for verification

|  | Floor space | Height | Flow rate of Methane gas | Ventilation rate | Density of Methane gas | Density of air |
|---|---|---|---|---|---|---|
| under the conditions witventilation | 0.136 [m2] | 0.3 [m] | $1.91 \times 10^{-6}$ [m³/s] | 1.7 [time/h] | 0.68 [kg/m3] | 1.22 [kg/m³] |

Results show that, with ventilation applied, accuracy declined near the floor, while empirical results are reproduced near the ceiling with the same accuracy as the CFD tools. Therefore, using this fast analysis tool, gas behavior near to ceilings can be quickly analyzed.



B2



B4

B6
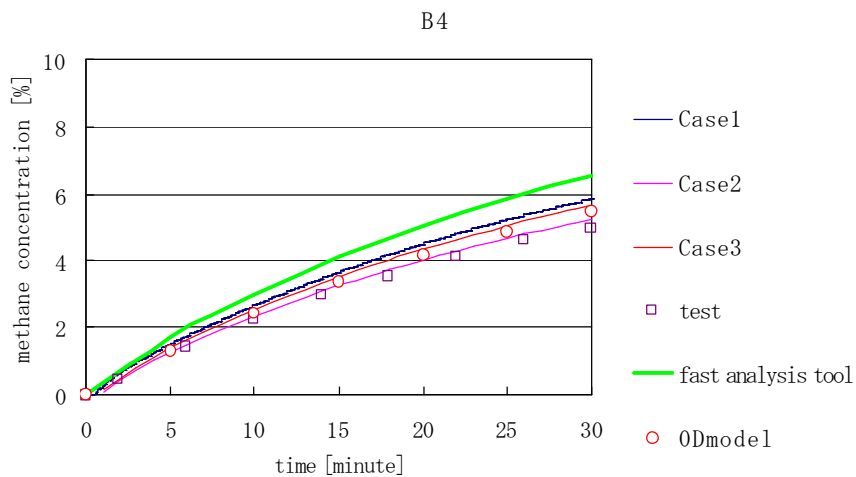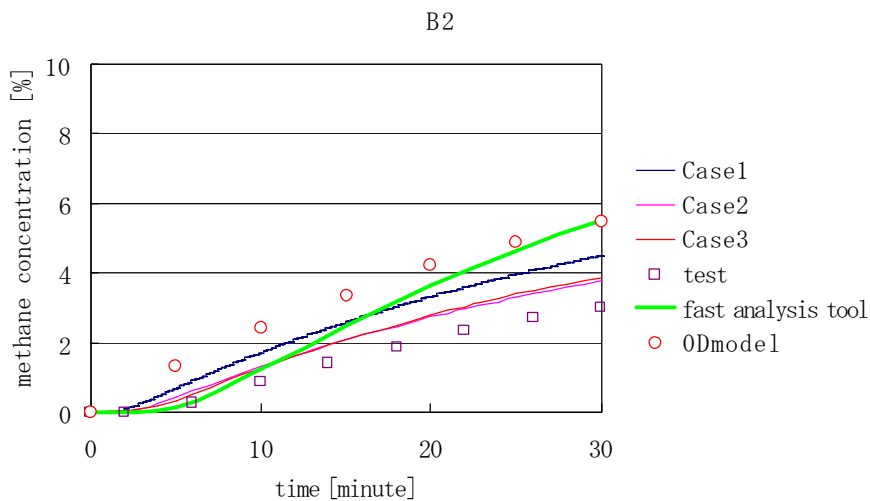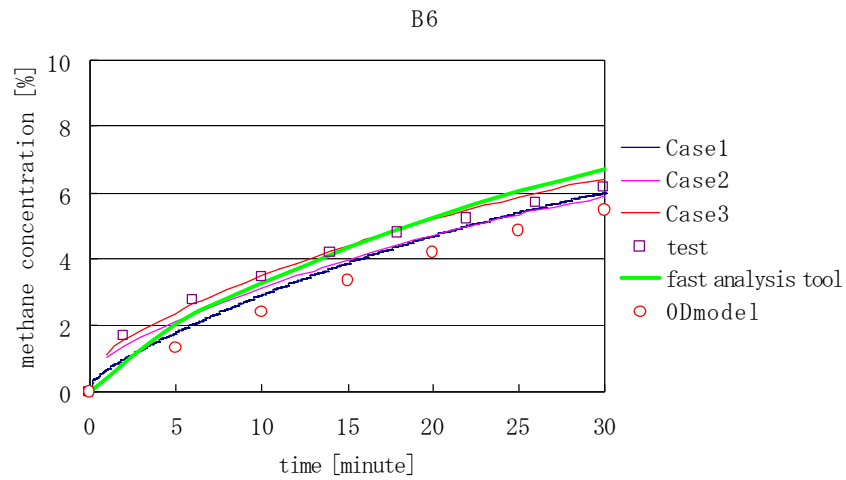


Figure11　The accuracy of fast analysis tool

## 5. Summary

This paper has discussed research conducted by the three gas utilities of Tokyo Gas, Osaka Gas and Toho Gas, aimed at establishing technologies for analyzing gas diffusion behavior.

The results of this research work are as follows.

・It is clarified that, by modeling with the CFD tools used by the three companies and appropriately setting parameters, gas diffusion behavior can be reproduced with an accuracy error of about 10%.

・It was confirmed that gas diffusion behavior in the full scale tests could be successfully reproduced under the similarity law.

・Knowing that gas concentration stays uniform in the horizontal direction as gas diffuses, a fast analysis tool that enables quicker analyses was created.

These analysis technologies will be applied towards verifying indoor gas diffusion behavior in order to safely and stably supply city gas in the future.

Symbols

$D$     :Ventilation port height [m]

$d$     :Methane inlet diameter [m]

$E$     :Entrainment coefficient

$\boldsymbol{g}$     :Gravitational acceleration vector

$H$     :Box height [m]

$L$     :Box width [m]

$Ls$     :Ventilation port width [m]

$M$     :Average molecular weight of gas mixture

$Ma$     :Molecular weight of air

$Mg$     :Molecular weight of methane

$P$     :Pressure [Pa]

$Qg$     :Methane flowrate [m$^3$/s]

$Qv$     :Ventilation rate [m$^3$/s]

$Re$     :Reynolds number

$Ri$     :Richardson number

$Sc$     :Schmidt number

$U$     :Average flow velocity of methane [m/s]

$Uv$     :Average flow velocity e of air [m/s]

$u$     :Flow velocity in x direction [m/s]

$\boldsymbol{v}$     :Flowrate vector

$W$     :Box depth [m]

$w$     :uFlow velocity in z direction [m/s]

$X$     :Molar fraction: 0, Air:1, Methane

$Y$     :Mass fraction: 0, Air: 1, Methane

$\alpha$     :Density ratio

$\beta$     :Flow rate ratio

$\mu g$     :Viscosity coefficient of methane [μPas]

$\rho$     :Density (Concentration) [kg/m3]

$\rho g$     :Methane gas concentration [kg/m3]

$\rho a$     :Air concentration [kg/m3]

References

(1) Marshall, The effect of ventilation on the accumulation and dispersal of hazardous gases、Proceedings of the 4th Int. Symp. on Loss Prevention and Safety Promotion in the Process Industries(1983)

(2)Grae Worster & Herbert E. Huppert, Time-dependent density profiles in a filling box, J. Fluid Mech. (1983) vol. 132, pp. 457-466

(3)Panos N. Papanicolaou & E. John List, Investigations of round vertial turbulent buoyant jets, J. Fluid Mech. (1988), vol. 195, pp. 341-391